

PATTERNS OF THE DEFORMATION RELIEF IN Ni₃Fe ALLOY SINGLE CRYSTALS WITH LONG-RANGE ATOMIC ORDER

T. S. Kunitsyna, L. A. Teplyakova, and N. A. Koneva

UDC 669. 017. 539. 4

Patterns of evolution of plastic deformation macrofragmentation and localization in [1.8.12] Ni₃Fe ordered alloy single crystals under compression are investigated. A two-level character of the fragmentation is revealed. It is demonstrated that the onset and the evolution of the stage of linear hardening is caused by the secondary macrofragmentation of the plastic deformation with participation of shear and rotation.

Keywords: single crystal, deformation fragmentation and localization.

INTRODUCTION

Single crystals of FCC metals and alloys are characterized by significant inhomogeneity of plastic deformation. The concept of deformation scale levels [1] allows patterns of plastic deformation of single crystals to be described most completely and thus this inhomogeneity to be taken into account. However, there are only a few works (for example, see [2, 3]) in which attempts were undertaken to describe the behavior of loaded alloy single crystals in the entire range of scales physically associated with a single crystal. Obviously, this is caused by the necessity of carrying out an extensive experiment. The situation can be facilitated, if the experiment is performed for the material for which experimental data have already been obtained that allow the volume of research to be decreased and the volume of information obtained to be increased purposefully. In this respect, Ni₃Fe alloy single crystals are very suitable objects. The single crystals of this alloy oriented for single slip have been studied in detail on the *microlevel*. Patterns of forming shear zones have already been established for them, substructure types have been identified, their interrelations with stages of the plastic deformation curve have been established, and the hardening mechanisms have been revealed [4, 5]. However, the local volume of the material of single crystals studied on the microlevel was so small, that this inevitably caused the loss of the aim of studies on the scale of the entire sample. Investigation of the shear pattern on the macrolevel will allow one to overcome this shortcoming. The present work is aimed at experimental investigation of the shear pattern for the ordered Ni₃Fe alloy single crystals deformed by compression to establish patterns of shear organization on different scale-structural levels and to reveal their relationships with the deformation stages.

MATERIAL AND METHODS OF RESEARCH

We investigated Ni₃Fe alloy single crystals with long-range atomic order and deformation axis parallel to the [1.8.12] crystallographic direction favorable for the single slip. Samples were shaped as rectangular parallelepipeds with end faces parallel to the (6.1.0) and (2.10. $\bar{7}$) crystallographic planes. The ($\bar{1}11$) [101] primary system was the most loaded slip system. The samples with sizes 3 × 3 × 6 mm were deformed by compression at room temperature with a rate of 1.5 · 10⁻² s⁻¹. Special measures on preservation of orientation of the compression axis (graphite greasing of the end faces) were undertaken. This requirement was controlled using epigrams taken before and after deformation that

Tomsk State University of Architecture and Building, Tomsk, Russia, e-mail: kma11061990@mail.ru. Translated from *Izvestiya Vysshikh Uchebnykh Zavedenii, Fizika*, No. 3, pp. 70–74, March, 2015. Original article submitted January 16, 2015.

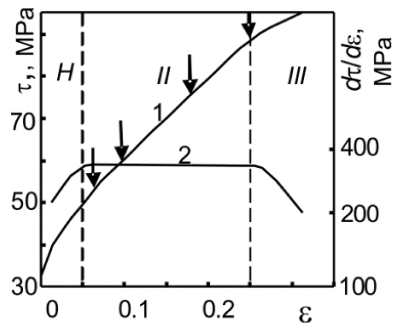


Fig. 1

Fig. 1. Dependence of the flow stress τ (curve 1) and of the strain hardening coefficient $d\tau/d\varepsilon$ (curve 2) on the strain ε .

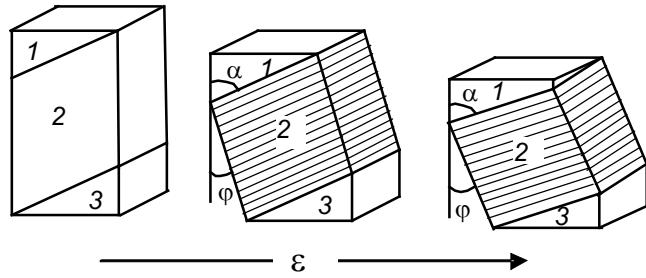


Fig. 2

Fig. 2. Deformation of the sample shape with strain.

demonstrated a certain degradation of the orientation. Nevertheless, the sample shapes after deformation demonstrated that they were deformed mainly along the primary slip plane in the entire strain range. The deformation relief was investigated using a MIM-10 optical microscope with 250 \times magnification.

RESULTS OF EXPERIMENT AND DISCUSSION

The dependence of the reduced stress (τ) on the strain (ε) for the examined single crystals is shown in Fig. 1. Using the dependence of the strain hardening coefficient ($\theta = d\tau/d\varepsilon$) on the strain (Fig. 1), the following stages were identified on curves $\tau(\varepsilon)$: unsteady slip stage (*H*) and linear hardening stage (II) transforming into stage III with decreasing θ for further strain increase. Transition to stage III occurred at $\varepsilon \approx 0.25$. The arrows above the curve indicate the points corresponding to the strain degrees at which the deformation relief was investigated.

Formation of the slip macroband. The deformation of the sample with the plastic strain is illustrated by Fig. 2. It can be seen that on the macrolevel, the deformation is localized in a geometrically localized volume. This volume was observed from the very onset of the plastic strain as dislocation slip along the primary planes unbounded by the end faces (fig. 2), that is, it represented the facilitated shear volume [3]. From the very onset of the plastic deformation, the single crystal is subdivided into three macrofragments: two end-face fragments and the central fragment (Fig. 2) in which the slip macroband is formed with further increase of strain. During plastic strain, the central macrofragment is deformed (Fig. 2). The angle φ , shown in Fig. 2, increases. In the beginning of stage II, $\tan\varphi = \gamma$, where γ is the shear strain. In turn, $\gamma \approx 2\varepsilon$ for small ε [6]. From this it follows that in the beginning of stage II, the deformation is provided mainly by the shear along the primary plane. With increasing strain degree and hence angle φ , this equality is violated. This means that other slip systems and, probably, other deformation regimes participate in deformation.

As demonstrated an analysis of the pattern of slip traces formed on the surface of faces of the three macrofragments, in the beginning of stage II the region of the macroband localization was not misoriented relative to the neighboring macrofragments 1 and 3. In particular, this is confirmed by the fact that angles α between the slip traces along the primary plane and the loading axis on the surface of all (three) macrofragments coincided. From the geometry of single crystals, this angle should be equal to 53 $^\circ$, which was the case for small strain degrees. With increasing strain degree, the angle α in the central macrofragment increased reaching $\sim 60^\circ$ by the end of stage II. This fact testified to the reorientation of the central macrofragment. Thus, during plastic deformation of the [1.8.12] single crystals of the ordered Ni₃Fe alloy, the primary macrofragmentation of the shear strain was observed [7] and its localization in the macroband whose linear sizes were commensurable with single crystal sizes.

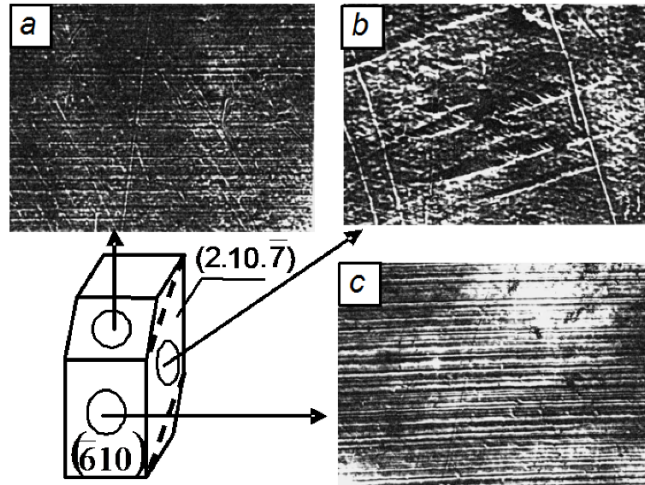


Fig. 3. Deformation relief in different regions of the surface of single crystal faces deformed to $\epsilon = 0.12$; $\times 250$.

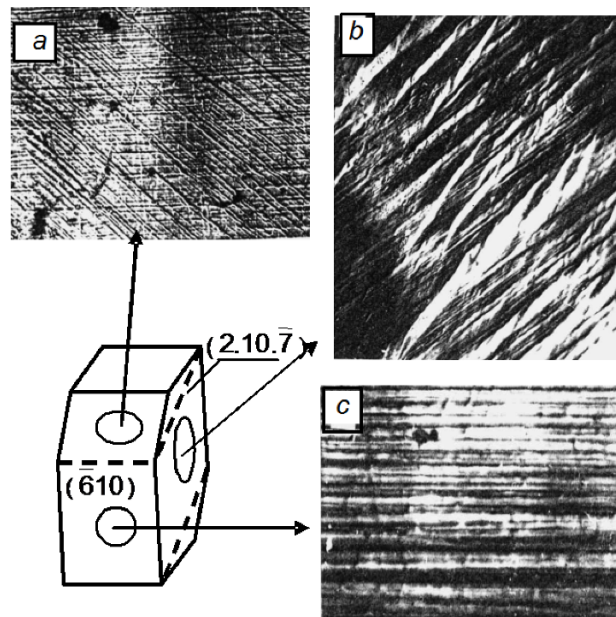


Fig. 4. Deformation relief in different regions of the surface of the single crystal deformed to $\epsilon = 0.25$; $\times 250$.

Evolution of the deformation relief. We note that the pattern of slip traces for the ordered alloy was characterized by low shear strength, and only the most severe traces were seen on the macrolevel. The shear on the $(2.10.\bar{7})$ face was so small that individual traces could not be resolved by the optical methods; therefore, main pieces of information at small ϵ were retrieved from the slip pattern formed on the $(\bar{6}10)$ face.

In the beginning of plastic strain the primary slip system acted in the entire sample, which was expected for the chosen orientation of single crystals, but the main part of primary slip traces was localized in the macroband (compare Fig. 3a and b). The traces belonging to this slip system were comparatively uniformly distributed in the macroband.

During entire stage II of the flow curve, the primary slip system continued to be active. This is illustrated by Figs. 3 and 4. Meanwhile, in the beginning of this stage several secondary slip systems participated in the strain. The

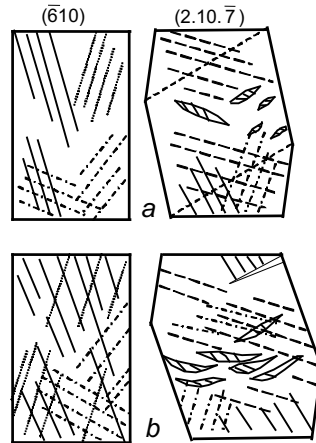


Fig. 5. Scheme of localization of the secondary slip plane traces on the single crystal surface at $\varepsilon = 0.12$ (a) and 0.25 (b).

density of the secondary slip traces in the end-face macrofragments was much higher than in the central fragment (compare Fig. 4a and c).

Figure 5a shows the schematic distribution of the secondary systems of slip traces for two perpendicular faces of the single crystal deformed to $\varepsilon = 0.12$. The slip traces along different planes are shown by lines of different types. It should be noted that the slip traces belonging to the cubic systems occupied equal regions of the surface with octahedral traces, which demonstrated high activity of the cubic slip already in the middle of stage II. The secondary slip traces were uniformly distributed in the region of manifestation of the cubic slip. With increasing strain degree, the relative fraction of the secondary slip increased, and by the end of stage II, it already encompassed the entire crystal (Fig. 5b). It can be seen that as a rule, 3–4 systems of slip traces are observed in local regions of the surface. However, different slip systems acted in different local volumes of the crystal, that is, macrofragmentation was characteristic as a whole on the macrolevel for the slip pattern which, as a matter of fact, was secondary in character [7].

Along with the slip, the process of reorientation of individual local crystal volumes relative to the initial crystal lattice was observed during plastic deformation of the [1.8.12] single crystals of the ordered Ni_3Fe alloy. As a result of this – secondary – reorientation, strain folds (Fig. 3b) are formed on the surfaces of the single crystal faces. The reorientation of local volumes is called secondary one because it is manifested for strain degrees higher than the primary one, and the scale of regions of the secondary reorientation is 10 times less. An analysis of the pattern of shear traces in the regions of fold edges performed in this work confirmed the reorientation (for example, see Fig. 3b). Attention was drawn to the fact that almost all folds were elongated in the direction that coincided with no one system of slip traces, octahedral or cubic ones, that is, they could not be formed by shear along these planes. Some folds had smooth (at least, on this scale level) surfaces, others were crossed by shear traces. The linear fold sizes were several hundred micrometers. Their boundaries were mainly rectilinear or slightly bent, though the boundaries of some folds were significantly bent (Fig. 3b). Almost all folds crossed the face, and their one or both ends were shaped as wedges. When the strain degree increased to that corresponding to the end of stage II, the crystal was deformed significantly, and the density of the strain folds in the central part of the faces increased significantly. They become the typical element of the deformation relief in the central macrofragment (Fig. 5b). The strain folds acquired more complicated, often helical shape (Fig. 4b). This demonstrated complication of the pattern of the internal long-range stress fields when several components of the bending-torsion tensor differed from zero [8].

A comparison of the results of investigation of the deformation relief on the macrolevel for the [1.8.12] single crystals of the Ni_3Fe alloy with short- [9] or long-range atomic order (SRO or LRO) allowed us to establish both their common features and significant differences. Thus, the deformation of the [1.8.12] single crystals of the Ni_3Fe alloy with LRO was analogous to that of the disordered alloy [9]. In single crystals of the alloy with LRO and SRO, the primary macrofragmentation of plastic deformation into three macrofragments occurred under compression. The

primary macrofragmentation in both alloys was caused by the identical initial single crystal geometries. The macrolocalization of plastic deformation in the geometrically isolated volume with the formation of the primary slip macroband also started from the very onset of the plastic deformation and developed during it. However, unlike the alloy with SRO, the reorientation of the macroband localization region (the central macrofragment) started for much lower strain degrees. Thus, the angle α in the LRO alloy reached 60° at $\varepsilon = 0.17$, and in the SRO alloy, the reorientation started only from $\varepsilon = 0.25$. In the ordered alloy, the angle φ (Fig. 2) at the end of stage II exceeded by almost 10° the corresponding angle in the disordered alloy for comparable values of ε . This demonstrated different mechanisms of deformation of single crystal of the alloys with LRO and SRO. In the ordered alloy, the beginning of stage II of the flow curve is associated with the participation in the deformation of several slip systems, rather than one as in the disordered alloy. In other words, patterns of the secondary macrofragmentation in the identically oriented Ni_3Fe alloy single crystals with LRO and SRO have significant differences. Unlike the SRO alloy, all octahedral and two cubic slip systems act in the ordered alloy already in the middle of stage II. The cubic systems in the SRO alloy act exclusively in the end-face macrofragments, that is, as a matter of fact, they are accommodation systems. The foregoing explains a higher strain hardening coefficient in stage II in the ordered alloy compared to the disordered alloy during any of the two stages of linear hardening [3].

CONCLUSIONS

1. The primary and secondary macrofragmentation of the shear strain was observed in the [1.8.12] single crystals of the ordered Ni_3Fe alloy under compression.

2. The primary macrofragmentation was due to slip strongly localized in the macroband; as a result, the single crystal was separated into three macrofragments: the central fragment (macroband) and two end-face fragments. With further increase of strain during stage II, the reorientation of the central macrofragment relative to the end-face fragments was observed.

3. The secondary macrofragmentation was due to the shear along all secondary octahedral and two cubic slip planes. Its occurrence correlated with the onset of the linear hardening stage and was one of the main reasons for high strain hardening coefficient observed in this stage.

4. The evolution of stage II was accompanied by the occurrence in the central macrofragment – the shear macroband – of local reorientation regions whose scale was in the range several tens – several hundreds of micrometers.

5. Creation of the long-range atomic order in the Ni_3Fe alloy led to another pattern of incorporation of secondary slip systems into strain and earlier occurrence of local misorientation volumes on the two scale levels.

REFERENCES

1. V. E. Panin, Yu. V. Grinyaev, T. F. Elsukova, and A. G. Ivanchin, *Russ. Phys. J.*, **25**, No. 6, 479–497 (1982).
2. L. A. Teplyakova, T. S. Kunitsyna, V. A. Starenchenko, and Poltaranin, *Russ. Phys. J.*, **57**, No. 4, 206–215 (2014).
3. L. A. Teplyakova and É. V. Kozlov, *Fizich. Mezomekh.*, **8**, No. 6, 57–66 (2005).
4. T. S. Kunitsyna, L. A. Teplyakova, and N. A. Koneva, *Adv. Mater. Res.*, **1013**, 54–61 (2014).
5. N. A. Koneva and É. V. Kozlov, *Russ. Phys. J.*, **33**, No. 2, 165–179 (1990).
6. R. W. K. Honeycomb, *Plastic Deformation of Metals* [Russian translation], Mir, Moscow (1974).
7. D. V. Lychagin and L. A. Teplyakova, *Pis'ma Zh. Tekh. Fiz.*, **29**, No. 12, 68–73 (2003).
8. M. A. Shtremel', *Strength of Alloys. Defects of the Lattice* [in Russian], Metallurgiya, Moscow (1982).
9. L. A. Teplyakova, T. S. Kunitsyna, N. A. Koneva, and É. V. Kozlov, *Fizich. Mezomekh.*, **3**, No. 5, 77–82 (2000).